Geophysical Research Letters

Key Points:
- We present the first in situ measurements of an explosive polarcyclone crossing the Antarctic marginal ice zone
- Warm air advection and wave propagation contribute to the maintenance of an unconsolidated sea ice surface far away from the ice edge
- Polar cyclones reshape the ice-covered ocean, thus extending the marginal ice zone beyond current definitions

Supporting Information:
- Supporting Information S1
- Movie S1

Correspondence to:
M. Vichi,
marcello.vichi@uct.ac.za

Effects of an Explosive Polar Cyclone Crossing the Antarctic Marginal Ice Zone

Marcello Vichi[1,2] (iD), **Clare Eayrs**[3] (iD), **Alberto Alberello**[4,5] (iD), **Anriëtte Bekker**[6] (iD), **Luke Bennetts**[4] (iD), **David Holland**[3,7] (iD), **Ehlke de Jong**[1], **Warren Joubert**[8] (iD), **Keith MacHutchon**[9], **Gabriele Messori**[10,11] (iD), **Jhon F. Mojica**[3] (iD), **Miguel Onorato**[12,13] (iD), **Clinton Saunders**[6], **Sebastian Skatulla**[9] (iD), **and Alessandro Toffoli**[5] (iD)

[1]Department of Oceanography, University of Cape Town, Cape Town, South Africa, [2]Marine Research Institute, University of Cape Town, Cape Town, South Africa, [3]Center for Global Sea Level Change, New York University Abu Dhabi, Abu Dhabi, United Arab Emirates, [4]School of Mathematical Sciences, University of Adelaide, Adelaide, South Australia, Australia, [5]Department of Infrastructure Engineering, The University of Melbourne, Parkville, Victoria, Australia, [6]Sound and Vibration Research Group, Department of Mechanical and Mechatronic Engineering, Stellenbosch University, Stellenbosch, South Africa, [7]Center for Atmosphere Ocean Science, Courant Institute of Mathematical Sciences, New York University, New York, NY, USA, [8]South African Weather Service, Pretoria, South Africa, [9]Department of Civil Engineering, University of Cape Town, Cape Town, South Africa, [10]Department of Earth Sciences, Uppsala University, Uppsala, Sweden, [11]Department of Meteorology and Bolin Centre for Climate Research, Stockholm University, Stockholm, Sweden, [12]Dipartimento di Fisica, Università di Torino, Turin, Italy, [13]INFN, Sezione di Torino, Turin, Italy

Abstract Antarctic sea ice shows a large degree of regional variability, which is partly driven by severe weather events. Here we bring a new perspective on synoptic sea ice changes by presenting the first in situ observations of an explosive extratropical cyclone crossing the winter Antarctic marginal ice zone (MIZ) in the South Atlantic. This is complemented by the analysis of subsequent cyclones and highlights the rapid variations that ice-landing cyclones cause on sea ice: Midlatitude warm oceanic air is advected onto the ice, and storm waves generated close to the ice edge contribute to the maintenance of an unconsolidated surface through which waves propagate far into the ice. MIZ features may thus extend further poleward in the Southern Ocean than currently estimated. A concentration-based MIZ definition is inadequate, since it fails to describe a sea ice configuration which is deeply rearranged by synoptic weather.

Plain Language Summary The extent of Antarctic sea ice is characterized by large regional variations that are in stark contrast with the alarming decreasing trends found in the Arctic. This is partly due to the presence of severe weather events, like extratropical cyclones travelling through the Southern Ocean and reaching the marginal ice zone (MIZ). The MIZ is a region where the ocean, atmosphere, and sea ice processes are closely interlinked. We provide direct evidence of how winter polar cyclones rearrange the MIZ and how their effects extend into the ice-covered region as far as the Antarctic continent. We present the first observations of large ice drift, ice concentration, and temperature changes as an explosively deepening cyclone crosses the MIZ. This case study is complemented by analysis of subsequent but more frequent storms that confirms how storminess in the Southern Ocean maintains a sea ice surface that is less compact, more mobile, and more extended than previously anticipated. Our results urge the scientific community to revise the current definition of the MIZ and improve its representation in models to better include the role of polar cyclones in detecting Antarctic sea ice trends.

1. Introduction

The ocean around Antarctica is home to some of the most severe storms on Earth. The majority of these are middle- and high-latitude synoptic cyclones, with a radius ranging from 500 to 2,000 km (Hoskins & Hodges, 2005; Uotila et al., 2011). Cyclones develop primarily in the Atlantic and Pacific sectors (Grieger et al., 2018; Hoskins & Hodges, 2005; Uotila et al., 2011; Wei & Qin, 2016; Yuan et al., 2009) and typically follow a south-eastward trajectory, undergoing net cyclogenesis in the midlatitudes and net cyclolysis closer to the Antarctic continent. The South Atlantic, and especially the ice-covered eastern Weddell Sea, is an area of net cyclolysis for systems originating from open ocean (Hoskins & Hodges, 2005; Yuan et al., 2009). The

highest density of intense cyclones occurs in winter in the Atlantic, with good agreement among the different storm tracking methods (Grieger et al., 2018).

These synoptic cyclonic systems contribute to the general atmospheric circulation in the Southern Ocean (Maksym, 2019; Simmonds, 2003). It is estimated that between 60% and 90% of the strong precipitation events in the region are due to synoptic systems (Papritz, Pfahl, Rudeva, et al., 2014), and cyclones modify the ocean, sea ice, and surface heat fluxes (Bracegirdle & Kolstad, 2010; Papritz, Pfahl, Sodemann, et al., 2014; Uotila et al., 2011). Cyclones are well-known vehicles of moisture and heat to the high latitudes (Messori et al., 2017; Woods & Caballero, 2016), and the regions of increased moisture flux south of 60°S in the Atlantic are related to the occurrence of strong cyclonic activity (Grieger et al., 2018). Synoptic systems also generate energetic waves in the Southern Ocean, and despite the higher number of cyclones during winter, waves are barely affected by seasonality (Young et al., 2011). Waves penetrate hundreds of kilometers into the sea ice-covered ocean (Kohout et al., 2014). Concomitantly, the ice cover attenuates the wave energy over distance, so that wave impacts die out eventually (Dolatshah et al., 2018).

Despite the continued study of extratropical cyclones (Schultz et al., 2018), our understanding of their interactions with sea ice is incomplete. The bulk of the literature has focused on the Arctic and on the impact of cyclones on ice concentration changes (Brümmer et al., 2008; Itkin et al., 2017; Kriegsmann & Brümmer, 2014; Lammert et al., 2009; Rae et al., 2017; Wei et al., 2019), recently including waves (Collins et al., 2015; Smith et al., 2018; Wang et al., 2016). In the Antarctic, where the ocean state and ice conditions are different, waves have been the main focus (Doble & Bidlot, 2013; Kohout et al., 2014). The few studies investigating the synoptic impacts on sea ice are of pack ice conditions in the Western Weddell Sea (e.g., Kottmeier & Sellmann, 1996; Uotila et al., 2000) or during summer (Wang et al., 2014).

Several works have indicated that Southern Hemisphere storminess may be a major driver of the trends (or lack thereof) observed in Antarctic sea ice extent (Maksym, 2019; Matear et al., 2015; Pezza et al., 2012; Schemm, 2018; Schlosser et al., 2018; Turner et al., 2017). Climate models struggle to capture this regional and temporal variability (Hobbs et al., 2014; Lecomte et al., 2016; Zunz et al., 2013), as well as the timing of the winter expansion and summer retreat (Hobbs et al., 2014). Different regions have shown a combination of positive and negative trends, whose significance is linked to the choice of statistical analyses (Yuan et al., 2017). Part of the dilemma on what is driving changes in Antarctic sea ice has been attributed to these opposing trends, thus reducing the consensus on a large-scale mechanism (Hobbs et al., 2016; Matear et al., 2015). This has become even more puzzling since 2016, when satellites recorded a substantial decrease in sea ice extent that counterbalanced the positive trend of the previous years (Maksym, 2019). Forced variability linked to climate modes such as the tropical El Niño-Southern Oscillation and the Southern Annular Mode may explain spring and autumn sea ice extent trends in certain regions, although the role of unforced, weather-dependent variability is usually invoked to justify the more modest correlations in other regions (Matear et al., 2015; Pezza et al., 2012; Stuecker et al., 2017).

A large portion of Antarctic sea ice natural variability seems to be linked to synoptic cyclones. However, large knowledge gaps still exist. Specifically, the effects of a polar cyclone crossing the marginal ice zone (MIZ) are yet unknown. The MIZ is the highly dynamic outer belt of (partially) ice-covered ocean formed by unconsolidated or broken ice (Doble et al., 2003; Wadhams et al., 1987, 2004), where open-ocean processes remain significant and cyclones potentially have large impacts on ice dynamics. It is usually identified in remotely sensed data as the region in which sea ice concentration falls between 15% and 80% (Stroeve et al., 2016; Strong & Rigor, 2013), although this definition is not based on dynamical considerations. The local air-sea exchanges of heat and momentum are affected by the presence of mixed sea ice conditions, from complete insulation in closed pack ice to the less-known interactions involving frazil and pancake ice (Alberello et al., 2019). The scarcity of data on winter sea ice drift and concentration in the Southern Ocean MIZ makes satellite imagery products the only source of information. These data sets have been mostly validated in the Arctic and are better suited for understanding large-scale and longer-term drift patterns (Kwok et al., 2017) rather than the characteristics of daily and subdaily ice motion, which are more likely affected by the passage of cyclones.

This letter presents the first quantitative evidence of the impact of polar cyclones on the Southern Ocean MIZ during winter conditions. Through the analysis of an explosive extratropical cyclone crossing the MIZ and of four subsequent polar cyclones of various intensity, we highlight the substantial role of storms
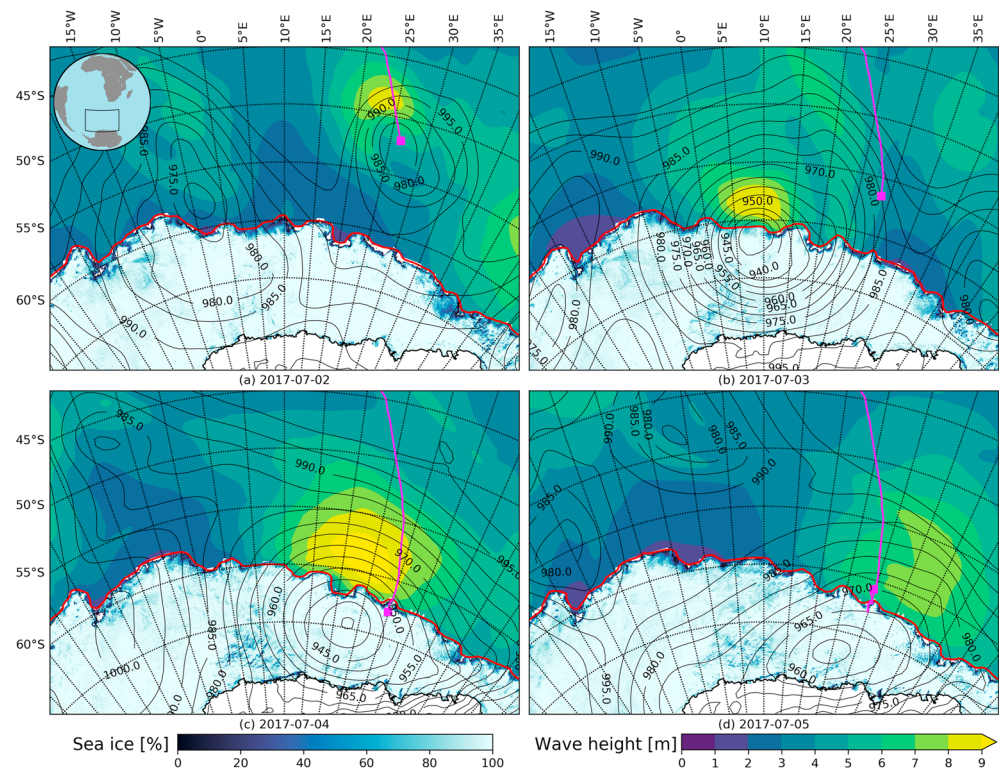
Figure 1. Evolution of the environmental conditions during the storm event (panels a–c show the conditions on 2–5 July 2017 respectively). Each panel shows mean sea level pressure (black lines, interval 5 hPa), significant wave height (colored shading, interval 1 m), and 15% sea ice concentration (red line), all from the ERA5 data set; sea ice concentration (black-blue-white shading, in percentage) from the AMSR2 ASI algorithm; and the ship track and location (purple line). All data are at 12:00 GMT on each day except the ERA5 sea ice margin, which is updated daily at midnight and is representative of the previous day.

in reshaping the MIZ, making the case for a much larger impact on the ice-covered ocean than previously anticipated.

2. In Situ Observations and Reanalysis Data

In situ sea ice data were collected from the SA Agulhas II research vessel along the WOCE I06 transect (Talley, 2013) between 1 and 20 July 2017 (Figure 1). Data consist of meteorological ship measurements, sea ice observations, and data from ice-tethered autonomous devices. Ship-based wind observations have been corrected to 10-m height according to specifications from the World Meteorological Organization (WMO, 2014). Sea ice observations (De Jong et al., 2018) followed the Antarctic Sea Ice Processes and Climate protocol. Visual observations have been integrated with data from ship-mounted cameras (Alberello et al., 2019). They captured the size of pancake ice floes encountered in the MIZ during the voyage, and gave accurate estimates of the area covered by solid ice, as opposed to interstitial slush. Autonomous devices were deployed on ice floes close to 62.8°S and 29.8°E on 4 July 2017 at about 100 km from the closest ice edge: Two Waves In Ice Observation Systems (NYU1-2, Eayrs et al., 2019) recorded position, temperature, and wave spectral characteristics every 15 min (Kohout et al., 2015), and three Trident Sensors Helix beacons (U1-3, Machutchon et al., 2019) transmitted their location every 4 hr. Both types of instrument were nonfloating devices and their positions were used to infer sea ice drift speed. Temperature profiles were taken alongside the deployments to estimate the oceanic heat flux. The NYU1 Waves In Ice Observation Systems failed after a few days, and its data will not be analyzed; the analysis period is from 4 to 20 July 2017, when NYU2 also ceased to transmit.

The in situ observations were integrated with earth observations products and climate reanalysis data from the European Centre for Medium-range Weather Forecast (ECMWF), as detailed in supporting information Text S1. Sea ice concentration data at high spatial resolution have been obtained from passive

microwave sensors AMSR2 (Advanced Microwave Scanning Radiometer 2, Spreen et al., 2008) and complemented by low-resolution sea ice drift product from EUMETSAT OSI SAF. Larger-scale meteorological and climatic conditions were obtained from ERA-Interim and ERA5, also using simulated wave data from the embedded WAM model (WAve Model, WAMDI Group, 1988), which does not resolve wave propagation in the MIZ. The atmospheric variables measured along the cruise track compared very well with the corresponding data from reanalyses (Figure S1), especially for mean sea level pressure; near-surface temperature and wind reanalyses data have been bias-corrected (see Text S1).

3. Results

3.1. Synoptic and MIZ Features

According to ERA5, a cyclonic structure developed around midday on 2 July at the sea ice edge (Figure 1). It progressed southeastward toward the Antarctic continent with a rapid deepening of the low-pressure core until complete lysis on the ice after 5 July. The minimum pressure found along the track simulated by ERA5 was 927 hPa (Figure 2a and S2), which is in the top 1% of winter cyclones in the climate reanalyses (Grieger et al., 2018; Wei & Qin, 2016) and a very rare low pressure condition over the winter Antarctic sea ice ($p < 0.01\%$, Figure S3). The corrected ERA5 maximum wind speed was greater than 33 m/s, while the sustained 1-min wind at the ship location was very close to that threshold (Figure 2a). Over the study period, four additional cyclones of various intensity impacted the region and will be compared to the first event (Figure S2; cyclones have been numbered from 1 to 5, with cyclone 1 being the main event depicted in Figure 1). Three out of the five cyclones were explosive events, indicated by the normalized deepening rates —the change in central pressure over 24 hr weighted by latitude—larger than 1 (Sanders & Gyakum, 1980; Lim & Simmonds, 2002; see Text S2). Cyclone 1 was characterized by explosive features when the core was well into the sea ice. All five cyclones can be classified as strong systems (Text S2), although their impact on the sea ice was different, as detailed in section 3.2.

The winter MIZ in this region of the Eastern Weddell Sea has not been sampled before, and its surface features were unknown. The combined sea ice observations shown in Figure 2b were obtained in the first 100 km from the ice edge, where the remote sensing concentration was above the 80% value that operationally identifies the upper limit of the MIZ. The ice edge is well identified by the satellite data, as generally found at the larger scale for winter conditions in the Southern Hemisphere (Worby & Comiso, 2004). However, our in situ data revealed that the satellite product cannot distinguish the ice cover characteristics. Our sea ice detection algorithm (Alberello et al., 2019) indicated that the surface was unconsolidated and comprised of ~50% pancakes for the whole sea ice transect, with frazil ice filling the interstitial gaps. This was confirmed by the Antarctic Sea Ice Processes and Climate observations that distinguished primary and secondary ice (Figure 2b and Movie S1; the variability of the visual observations is an indication of the subjectivity in determining the relative composition of sea ice in a complex configuration). While the satellite returned a technically correct 100% concentration due to the full coverage of the ocean by solid floes and frazil ice, our measurements highlight the rashness of equating this to consolidated ice.

3.2. Locally Measured Impacts on Sea Ice

Figure 2c shows that warmer air temperatures were observed on sea ice when the explosive first cyclone was closest to the buoy location, and this also happened for the subsequent storms. The reanalyzed temperatures correlate well with the observations, which supports our use of the reanalyses for studying the larger-scale features. During all events, air temperature increased rapidly to values close to melting and then returned to −15 °C in ~2 days. Cyclone 1 was characterized by a longer duration of anomalous warmer temperatures. In Figure 2e, we compare the climatological daily anomaly following the cyclone cores with that computed at the location of the reference NYU2 buoy. The warm core anomaly is evident in all storms, but cyclone 1 is the only one with a stable anomaly of about +5 °C throughout the track. The cyclone 1 warm core extended vertically up to 800 hPa and persisted deep into the sea ice until 5 July (Figure S4). The temperature anomaly at the sea ice buoy always peaks when the low pressure system is close (Figure 2e), independent of the storm intensity, although there is no clear relationship between distance from the cyclone, core temperature, and the related temperature increase on ice.

During all cyclones but the last, both the ice drift speed and the wave height in the MIZ increased (Figures 2d and 2f). The increase in ice drift was observed after about 1 day, and it was almost identical for all the buoys
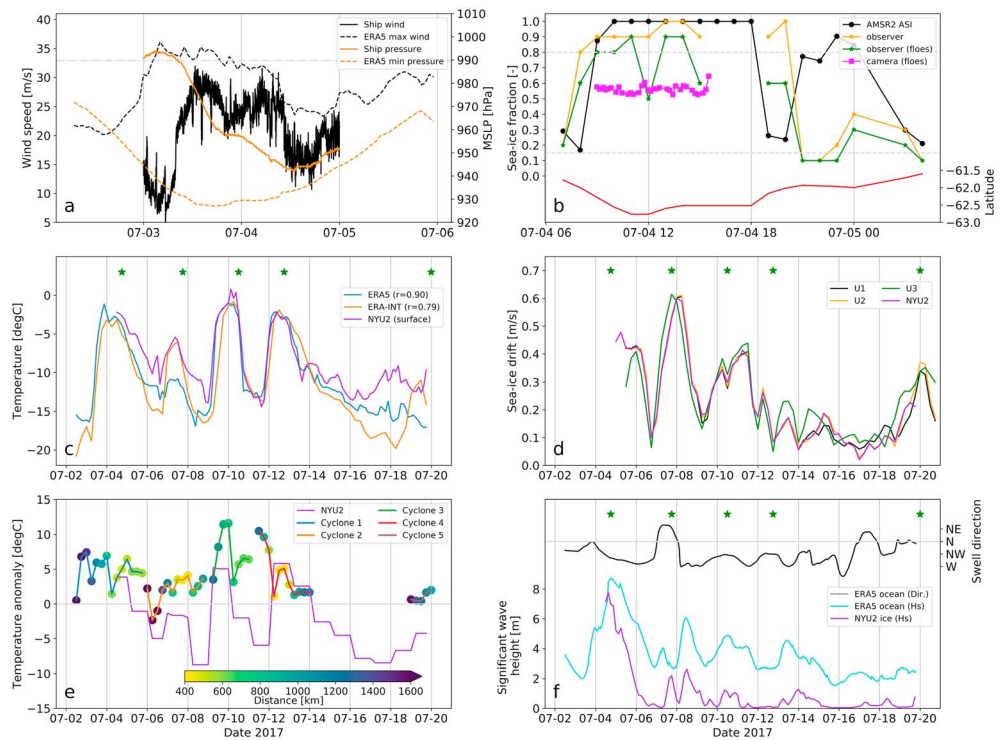
Figure 2. (a, b) Ship-based observations during the explosive cyclone (cyclone 1). (a) Shipborne atmospheric measurements of sustained wind and mean sea level pressure (MSLP) during the cyclone (1-min averages) at the ship location, compared with the ERA5 minimum central pressure and bias-corrected maximum wind speed along the cyclone track (Text S1). See Figure S1 for the analysis of collocated ship and reanalyses data. The dashed gray line is the threshold used for category 1 tropical cyclones. (b) Sea ice concentration in the marginal ice zone observed from remote sensing (AMSR2 ASI), Antarctic Sea Ice Processes and Climate visual observations (total and pancake ice floe concentration), and automatic cameras (pancake ice floe; Alberello et al., 2019). The dashed gray lines indicate the operational thresholds of the marginal ice zone (15–80%). The red line at the bottom shows the latitudes following the track shown in Figure S5. (c–f) In situ observations of the five cyclones. (c) Atmospheric temperature from the Waves In Ice Observation Systems buoy NYU2 and the ECMWF reanalyses. The linear correlation coefficients are reported in the legend, and the star symbols indicate the time when the storm cores were the closest to the buoy location (see panel e); (d) sea ice drift speed measured at the location of the ice-tethered buoys; and (e) atmospheric temperature anomaly with respect to the ERA-Interim climatology at the location of the NYU2 buoy and in the cores of the storms during the investigated period (the trajectory is shown in Figure S1). The distance of the storm cores from the buoy location is indicated by the colored circles; and (f) open-ocean significant wave height and swell direction simulated by ERA5 compared to the significant wave height measured by the NYU2 buoy on sea ice. Data are presented as averages over 3 hr when comparing with ERA5 and over 6 hr for ERA-Interim.

in the array, suggesting free drift conditions. The floes in the frazil-pancake field were not moving relative to one another at scales between 5 and 100 km. Interestingly, the largest drift was not measured during cyclone 1 but rather in the subsequent storms that hit the MIZ. The swell was the most intense during cyclone 1, with a measured significant wave height (SWH) close to 8 m in sea ice and a slightly higher simulated value of 8.5 m in the open ocean. The WAM-predicted wave direction was north/northwest sector, which is in agreement with the visual observations following the WMO protocol. According to the model, SWH grew quickly in the open ocean close to the MIZ from 3 July, when the core of the cyclone was still 1,500 km away (Figure 2e). WAM does not compute wave propagation in sea ice, and thus, no wave motion is prescribed when ice concentration is above 30%. Since the satellite-derived ice concentration was 100% very close to the ice edge (Figure 2b), the model can only be used to infer the main characteristics of the incident wave field in the open ocean. Nevertheless, measured SWH on sea ice correlated very well for the entire 20 days with the simulated open-ocean wave field for a large region around the buoy location ($r > 0.8$, see Figure S6). We do not have enough data to assess wave attenuation in the MIZ, but we observe that there is always wave energy present and that it was the highest during cyclone 1. Waves in the MIZ were evident also during the period of storm quiescence after 14 July, when the atmospheric temperature
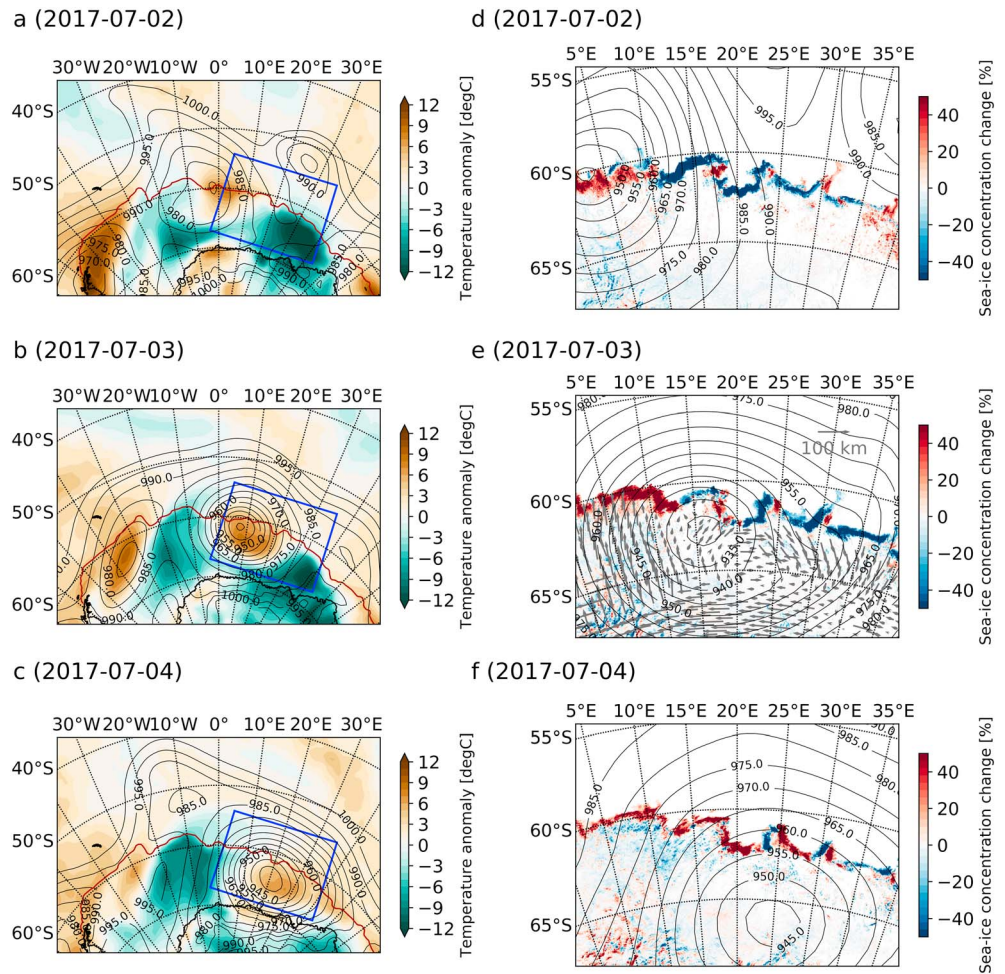
Figure 3. Multiple impacts of the explosive cyclone (cyclone 1) on surface features in the eastern Weddell Sea. (a–c) Daily anomalies of the surface atmospheric temperature over the period 2–4 July 2017 computed against the ERA-Interim climatology (1979–2017). The daily mean isolines of surface atmospheric pressure and 15% sea ice concentration are also shown from the same data set. The box indicates the region shown in the right column panels. (d–f) Details of the daily changes in sea ice concentration (mean concentration for the day minus the previous day's value) from AMSR2 ASI data in the boxed region of (a)–(c). The mean sea level pressure isolines from 00:00 GMT of 3–5 July 2017 are overlain for reference. (e) also shows the estimated ice displacement (in kilometers) over approximately 48 hr centered on 3 July from OSI-SAF.

decreased and the median distance of the buoy from the ice edge increased (Figures 2c and S6). This indicates that sea ice did not reach closed pack ice conditions at an average distance of 200 km from the edge but maintained MIZ characteristics despite satellite data indicating 100% concentration.

3.3. Impact of the Explosive Cyclone on the Wider MIZ

The region affected by cyclone 1 covers more than 2,000 km and extends far into the sea ice. This can be observed in the temperature anomaly and the associated synoptic low pressure systems from 2 to 4 July (Figure 3). The initial evolution of the daily near-surface temperature anomalies is similar to open-ocean midlatitude cyclones (Yuan et al., 2009): Warm air is advected poleward on the eastern side, while the equatorward cold front is found on the western side. The observed pattern of positive and negative temperature anomalies is associated with the concurrent presence of several cyclones (Figures 3a–3c). As supported by the data (see Figure 2), when the cyclone travels over the MIZ, it warms the overlying air temperature, generates waves close to the edge, pushes the edge on the downwind side poleward, and accesses the pool of cold air over the Antarctic continental margin (Figures 3b and 3c). The result of these processes is clearly visible in the daily changes of sea ice concentration detected by the high-resolution AMSR2 sensor (Figures 3d–3f). Although the satellite absolute concentration does not allow us to distinguish the extent of the MIZ, the
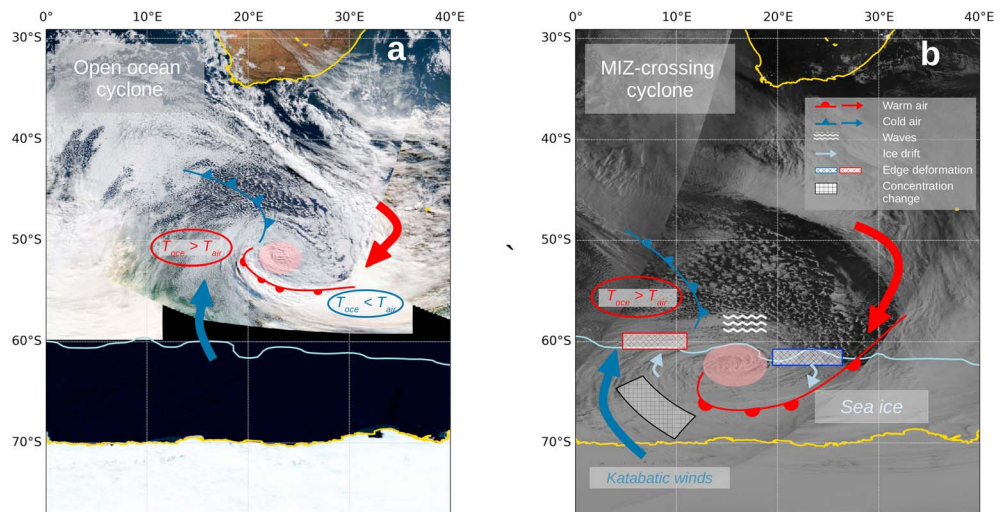
Figure 4. Schematic of a polar cyclone (a) on the open ocean (from Moderate Resolution Imaging Spectroradiometer, MODIS-Terra true color mosaic, 02 July 2017) and (b) when crossing the MIZ (from Visible Infrared Imaging Radiometer Suite, VIIRS nighttime imagery of Cyclone 1, 03 July 2017). The light blue contour is the daily 15% sea ice concentration as assimilated in ERA5. The location of the arrows, fronts, and warm core (the red elliptic region) with respect to the depicted storms is illustrative of their main features. The open-ocean case (a) presents air-sea interactions showing the expected relationship between the air temperature (T_{air}) and the ocean temperature (T_{oce}); this is not shown for the sea ice case (b) due to the less known interactions between air and sea ice under extreme events. MIZ = marginal ice zone.

relative change is an indicator of deformation. The changes in sea ice concentration are more evident at the edge of the ice-covered region affected by the intense winds and the advection of warm air. As the cyclone moves eastward, the MIZ concentration is rearranged in a clockwise rotation, with a clear zonal motion when the isobars are parallel to the edge, as highlighted by the large daily change seen at the tongues located at 25°E and 30°E. Due to the persistence of the cyclone over sea ice for about 3 days, the large-scale motion was also captured by the coarse ice displacement products from OSI-SAF (section 2.2 and Figure 3e), which is in very good agreement with the cyclone features. When cyclone 1 crosses the ice edge, there is no apparent deformation of ice in the interior: The upward increase observed on the western side is not balanced by a decrease poleward (the opposite happens on the eastern side). Being already saturated at 100%, the satellite images cannot measure any concentration change. As the storm progresses and the concurrent action of warmer air and waves in the sea ice, the wider, internal region is affected, with concentration changes of more than 20% very close to the Antarctic continent indicating ice rearrangement.

4. Discussion and Conclusions

The data presented here provide the first detailed in situ record of the impact of an explosive cyclone on the MIZ. Its track, which brought it to cross a wide expanse of the MIZ in the eastern Weddell Sea, makes it an ideal case study to further our understanding of atmosphere-ocean-sea ice interactions in this region. The agreement between our in situ measurements and ECMWF reanalysis products justified the use of climate reanalyses to study the evolution of metocean conditions as the extreme polar cyclone approached sea ice. Over the period of the instrument deployment, four subsequent storms affected the region, and their effects on sea ice were compared with the extreme event crossing the MIZ. These were still intense (Figures S2 and S3 and Text S2) and are more representative of "typical" winter storms in the region. We thus argue that high-latitude cyclonic systems, beyond extreme explosive events, have a continuous effect in reshaping the MIZ at synoptic scales.

Based on the extreme case study, Figure 4 provides a schematic diagram of the processes linked to an ice-landing polar cyclone, comparing them with what is known to happen in the open ocean. Extratropical cyclones in the open ocean (Figure 4a) contribute to the advection of warm, moist air poleward (Grieger et al., 2018). However, the net ocean-atmosphere heat flux is supposedly balanced by the ocean heat gain

in the warm sector and heat loss in the cold sector (Yuan et al., 2009). This picture is modified when the extratropical cyclones occur closer to the Antarctic continent, often leading to marine cold air outbreaks (Bracegirdle & Kolstad, 2010; Papritz, Pfahl, Sodemann, et al., 2014), which are known to strongly affect the heat fluxes closer to the sea ice. The interconnected processes occurring when polar cyclones cross the MIZ can be summarized as follows (Figure 4b): (i) advection of warm oceanic air onto the sea ice; (ii) intensified sea ice drift with larger synoptic ice edge deformation on the upwind and downwind flanks and concentration changes in the interior; and (iii) wave propagation into the sea ice for ~200 km while maintaining considerable energy. The extremeness of the studied event highlights the scale of the meridional heat advection on sea ice (Figure 3); the advected warm air remains framed in the cyclone core and affects sea ice all the way to the Antarctic coastline. The cold air outbreak observed in the analysis of the daily anomalies would only partly compensate the heat gain on the warm sector. The net effect on the ocean is likely to be cooling (Papritz, Pfahl, Sodemann, et al., 2014), although it was not possible to verify this through satellite data due to the intense cloud cover and further investigation on the oceanic impact is needed. After the passage of the cyclone, the air temperature on sea ice returns to freezing conditions, but the net impact on the ice surface is uncertain. We argue that these fluxes cannot be fully investigated by using the current reanalyses products since the representation of the assimilated ice surface based on satellite data is not accurate.

The largest drift speeds were observed during the cyclones (up to 0.75 m/s), and large portions of the edge of up to 100 km (the maximum distance between the buoys) moved coherently. Large drift speeds have been previously observed in winter in the Central Weddell Sea (Vihma et al., 1996) and spring in the Amundsen Sea (Ackley et al., 2015), which exceed the reported mean drift speed of 0.2–0.3 m/s (Doble & Wadhams, 2006). However, these studies had not related larger drift speeds to storm conditions, as demonstrated here. One implication of drift is enhanced ocean heat flux, which was on the lower end of the previous measurements (11 W/m^2, see Text S3; McPhee et al., 1999; Ackley et al., 2015); evidently, this extreme event did not enhance the upwelling of warmer waters, in contrast with what found in the Arctic (Smith et al., 2018).

The Arctic case studies presented in section 1 highlight the ice-cyclone interactions in terms of concentration changes: ice breakup and leads formation are followed by the drift increase and wave propagation (e.g., Collins et al., 2015; Itkin et al., 2017). In contrast, in the Southern Ocean, we suggest that the storm-driven wave propagation and oceanic air advection delay consolidation and maintain the mixed frazil-pancake field, also when ice concentration is close to 100%. This set of observations sheds a new light on sea ice features and their interaction with intense atmospheric events which differs from those previously observed in the Weddell Sea (Doble & Wadhams, 2006; Valkonen et al., 2008) and other Arctic cases (Collins et al., 2015; Itkin et al., 2017; Smith et al., 2018). Despite the ice edge moving away from the ice-tethered buoy over the 20 days period by 200 km, the surface was never consolidated, and the concurrent drift and wave motion were evident (Figures 2d–2f). The daily changes observed in the large ice-covered region affected by the cyclone (Figures 3d–3f) indicate the presence of unconsolidated ice farther away from the edge, which may also be caused by ice breakup.

The current concentration-based definition of MIZ extent as a narrow transitional region (from 15% to 80% ice concentration) is not compatible with our comprehensive set of observations. We notice that this is not due to a bias in the satellite estimates of ice concentration: The ocean is indeed fully ice-covered, but the surface morphology is not equivalent to pack ice conditions. This issue would be improved by the use of algorithms that allow discrimination of the various ice types as done in the Arctic (Ye et al., 2016) and by explicitly including floe sizes in numerical models (Roach et al., 2018). Young sea ice, at least in this region of the Southern Ocean, is not identified by the presence of some ice-free ocean but rather by the combination of floes and frazil ice. The characterization of air-sea ice exchanges in the presence of large fractions of frazil ice should be further investigated as much larger heat, momentum, and material fluxes may occur (e.g., Matsumura & Ohshima, 2015).

In addition to the climatic drivers contributing to the 2016 anomaly (Meehl et al., 2019; Stuecker et al., 2017), we suggest that given the evidence of how high-latitude cyclones determine the surface features of the MIZ and its effective extent, the unforced and thus unpredictable variability of the polar atmosphere at longer time scales will diminish our capability to predict sea ice extent trends. The many possible perspectives on the interpretation of the trends indicate that large synoptic high-latitude cyclones, and possibly mesoscale

events, may be major drivers of the natural variability of sea ice; the details as to how these processes are included in numerical models would become the discriminant for their predictive skills.

References

Ackley, S. F., Xie, H., & Tichenor, E. A. (2015). Ocean heat flux under Antarctic sea ice in the Bellingshausen and Amundsen Seas: Two case studies. *Annals of Glaciology*, *56*(69), 200–210. https://doi.org/10.3189/2015AoG69A890

Alberello, A., Onorato, M., Bennetts, L., Vichi, M., Eayrs, C., MacHutchon, K., & Toffoli, A. (2019). Brief communication: Pancake ice floe size distribution during the winter expansion of the Antarctic marginal ice zone. *The Cryosphere*, *13*(1), 41–48. https://doi.org/10.5194/tc-13-41-2019

Bracegirdle, T. J., & Kolstad, E. W. (2010). Climatology and variability of Southern Hemisphere marine cold-air outbreaks. *Tellus A: Dynamic Meteorology and Oceanography*, *62*(2), 202–208. https://doi.org/10.1111/j.1600-0870.2009.00431.x

Brümmer, B., Schröder, D., Müller, G., Spreen, G., Jahnke-Bornemann, A., & Launiainen, J. (2008). Impact of a Fram Strait cyclone on ice edge, drift, divergence, and concentration: Possibilities and limits of an observational analysis. *Journal of Geophysical Research - Oceans*, *113*, C12003. https://doi.org/10.1029/2007JC004149

Collins, C. O., Rogers, W. E., Marchenko, A., & Babanin, A. V. (2015). In situ measurements of an energetic wave event in the Arctic marginal ice zone. *Geophysical Research Letters*, *42*, 1863–1870. https://doi.org/10.1002/2015GL063063

Doble, M. J., & Bidlot, J.-R. (2013). Wave buoy measurements at the Antarctic sea ice edge compared with an enhanced ECMWF WAM: Progress towards global waves-in-ice modelling. *Ocean Modelling*, *70*, 166–173. https://doi.org/10.1016/j.ocemod.2013.05.012

Doble, M. J., Coon, M., & Wadhams, P. (2003). Pancake ice formation in the Weddell Sea. *Journal of Geophysical Research*, *108*(C7), 3209. https://doi.org/10.1029/2002JC001373

Doble, M. J., & Wadhams, P. (2006). Dynamical contrasts between pancake and pack ice, investigated with a drifting buoy array. *Journal of Geophysical Research*, *111*(C11). https://doi.org/10.1029/2005JC003320

Dolatshah, A., Nelli, F., Bennetts, L. G., Meylan, M. H., Alberello, A., Monty, J., & Toffoli, A. (2018). Hydroelastic interactions between water waves and floating freshwater ice. *Physics of Fluids*, *30*(9), 091702. https://doi.org/10.1063/1.5050262

Eayrs, C., Holland, D., Mojica, J., Vichi, M., Alberello, A., Bekker, A., et al. (2019, updated 2019) SA Agulhas II Winter 2017 Cruise: Waves In Ice Observation Systems (WIIOS) [Data set]. Australian Antarctic Data Centre. https://doi.org/10.26179/5cc934992f065

Grieger, J., Leckebusch, G. C., Raible, C. C., Rudeva, I., & Simmonds, I. (2018). Subantarctic cyclones identified by 14 tracking methods, and their role for moisture transports into the continent. *Tellus A: Dynamic Meteorology and Oceanography*, *70*(1), 1–18. https://doi.org/10.1080/16000870.2018.1454808

Hobbs, W. R., Bindoff, N. L., & Raphael, M. N. (2014). New perspectives on observed and simulated Antarctic sea ice extent trends using optimal fingerprinting techniques. *Journal of Climate*, *28*(4), 1543–1560. https://doi.org/10.1175/JCLI-D-14-00367.1

Hobbs, W. R., Massom, R., Stammerjohn, S., Reid, P., Williams, G., & Meier, W. (2016). A review of recent changes in Southern Ocean sea ice, their drivers and forcings. *Global and Planetary Change*, *143*, 228–250. https://doi.org/10.1016/j.gloplacha.2016.06.008

Hoskins, B. J., & Hodges, K. I. (2005). A new perspective on Southern Hemisphere storm tracks. *Journal of Climate*, *18*(20), 4108–4129. https://doi.org/10.1175/JCLI3570.1

Itkin, P., Spreen, G., Cheng, B., Doble, M., Girard-Ardhuin, F., Haapala, J., et al. (2017). Thin ice and storms: Sea ice deformation from buoy arrays deployed during N-ICE2015. *Journal of Geophysical Research: Oceans*, *122*, 4661–4674. https://doi.org/10.1002/2016JC012403

de Jong, E., Vichi, M., Mehlmann, C. B., Eayrs, C., De Kock, W., Moldenhauer, M., & Audh, R. R. (2018). Sea ice conditions within the Antarctic marginal ice zone in winter 2017, onboard the SA Agulhas II [Data set]. University of Cape Town. https://doi.org/10.1594/PANGAEA.885211

Kohout, A. L., Penrose, B., Penrose, S., & Williams, M. J. (2015). A device for measuring wave-induced motion of ice floes in the Antarctic marginal ice zone. *Annals of Glaciology*, *56*(69), 415–424. https://doi.org/10.3189/2015AoG69A600

Kohout, A. L., Williams, M. J. M., Dean, S. M., & Meylan, M. H. (2014). Storm-induced sea ice breakup and the implications for ice extent. *Nature*, *509*(7502), 604–607. https://doi.org/10.1038/nature13262

Kottmeier, C., & Sellmann, L. (1996). Atmospheric and oceanic forcing of Weddell Sea ice motion. *Journal of Geophysical Research - Oceans*, *101*(C9), 20809–20824. https://doi.org/10.1029/96JC01293

Kriegsmann, A., & Brümmer, B. (2014). Cyclone impact on sea ice in the central Arctic Ocean: A statistical study. *The Cryosphere*, *8*(1), 303–317. https://doi.org/10.5194/tc-8-303-2014

Kwok, R., Pang, S. S., & Kacimi, S. (2017). Sea ice drift in the Southern Ocean: Regional patterns, variability, and trends. *Elem Sci Anth*, *5*(0), 32. https://doi.org/10.1525/elementa.226

Lammert, A., Brümmer, B., & Kaleschke, L. (2009). Observation of cyclone-induced inertial sea-ice oscillation in Fram Strait. *Geophysical Research Letters*, *36*, L10503. https://doi.org/10.1029/2009GL037197

Lecomte, O., Goosse, H., Fichefet, T., Holland, P. R., Uotila, P., Zunz, V., & Kimura, N. (2016). Impact of surface wind biases on the Antarctic sea ice concentration budget in climate models. *Ocean Modelling*, *105*, 60–70. https://doi.org/10.1016/j.ocemod.2016.08.001

Lim, E.-P., & Simmonds, I. (2002). Explosive cyclone development in the Southern Hemisphere and a comparison with Northern Hemisphere events. *Monthly Weather Review*, *130*(9), 2188–2209. https://doi.org/10.1175/1520-0493(2002)130<2188:ECDITS>2.0.CO;2

Machutchon, K., Vichi, M., Eayrs, C., Alberello, A., Bekker, A., Bennetts, L., et al. (2019, updated 2019) AGULHAS_TRACKERS_2017 [Data set]. Australian Antarctic Data Centre https://doi.org/10.26179/5cc937513bd6d

Maksym, T. (2019). Arctic and Antarctic sea ice change: Contrasts, commonalities, and causes. *Annual Review of Marine Science*, *11*(1), 187–213. https://doi.org/10.1146/annurev-marine-010816-060610

Matear, R. J., O'Kane, T. J., Risbey, J. S., & Chamberlain, M. (2015). Sources of heterogeneous variability and trends in Antarctic sea ice. *Nature Communications*, *6*(1), 8656. https://doi.org/10.1038/ncomms9656

Matsumura, Y., & Ohshima, K. I. (2015). Lagrangian modelling of frazil ice in the ocean. *Annals of Glaciology*, *56*(69), 373–382. https://doi.org/10.3189/2015AoG69A657

McPhee, M. G., Kottmeier, C., & Morison, J. H. (1999). Ocean heat flux in the central Weddell Sea during winter. *Journal of Physical Oceanography*, *29*(6), 1166–1179. https://doi.org/10.1175/1520-0485(1999)029<1166:OHFITC>2.0.CO;2

Meehl, G. A., Arblaster, J. M., Chung, C. T. Y., Holland, M. M., DuVivier, A., Thompson, L., et al. (2019). Sustained ocean changes contributed to sudden Antarctic sea ice retreat in late 2016. *Nature Communications*, *10*(1), 14. https://doi.org/10.1038/s41467-018-07865-9

Messori, G., Woods, C., & Caballero, R. (2017). On the drivers of wintertime temperature extremes in the high Arctic. *Journal of Climate*, *31*(4), 1597–1618. https://doi.org/10.1175/JCLI-D-17-0386.1

Papritz, L., Pfahl, S., Rudeva, I., Simmonds, I., Sodemann, H., & Wernli, H. (2014). The role of extratropical cyclones and fronts for Southern Ocean freshwater fluxes. *Journal of Climate*, *27*(16), 6205–6224. https://doi.org/10.1175/JCLI-D-13-00409.1

Papritz, L., Pfahl, S., Sodemann, H., & Wernli, H. (2014). A climatology of cold air outbreaks and their impact on air–sea heat fluxes in the high-latitude South Pacific. *Journal of Climate*, *28*(1), 342–364. https://doi.org/10.1175/JCLI-D-14-00482.1

Pezza, A. B., Rashid, H. A., & Simmonds, I. (2012). Climate links and recent extremes in Antarctic sea ice, high-latitude cyclones, Southern Annular Mode and ENSO. *Climate Dynamics*, *38*(1-2), 57–73. https://doi.org/10.1007/s00382-011-1044-y

Rae, J. G. L., Todd, A. D., Blockley, E. W., & Ridley, J. K. (2017). How much should we believe correlations between Arctic cyclones and sea ice extent? *The Cryosphere*, *11*(6), 3023–3034. https://doi.org/10.5194/tc-11-3023-2017

Roach, L. A., Horvat, C., Dean, S. M., & Bitz, C. M. (2018). An emergent sea ice floe size distribution in a global coupled ocean-sea ice model. *Journal of Geophysical Research: Oceans*, *123*, 4322–4337. https://doi.org/10.1029/2017JC013692

Sanders, F., & Gyakum, J. R. (1980). Synoptic-dynamic climatology of the "bomb". *Monthly Weather Review*, *108*(10), 1589–1606. https://doi.org/10.1175/1520-0493(1980)108,1589:SDCOT.2.0.CO;2

Schemm, S. (2018). Regional trends in weather systems help explain Antarctic sea ice trends. *Geophysical Research Letters*, *45*, 7165–7175. https://doi.org/10.1029/2018GL079109

Schlosser, E., Haumann, F. A., & Raphael, M. N. (2018). Atmospheric influences on the anomalous 2016 Antarctic sea ice decay. *The Cryosphere*, *12*(3), 1103–1119. https://doi.org/10.5194/tc-12-1103-2018

Schultz, D. M., Bosart, L. F., Colle, B. A., Davies, H. C., Dearden, C., Keyser, D., et al. (2018). Extratropical cyclones: A century of research on meteorology's centerpiece. *Meteorological Monographs*, *59*, 16.1–16.56. https://doi.org/10.1175/AMSMONOGRAPHS-D-18-0015.1

Simmonds, I. (2003). Modes of atmospheric variability over the Southern Ocean. *Journal of Geophysical Research, Oceans*, *108*, SOV 5-1. https://doi.org/10.1029/2000JC000542

Smith, M., Stammerjohn, S., Persson, O., Rainville, L., Liu, G., Perrie, W., et al. (2018). Episodic reversal of autumn ice advance caused by release of ocean heat in the Beaufort Sea. *Journal of Geophysical Research: Oceans*, *123*, 3164–3185. https://doi.org/10.1002/2018JC013764

Spreen, G., Kaleschke, L., & Heygster, G. (2008). Sea ice remote sensing using AMSR-E 89-GHz channels. *Journal of Geophysical Research - Oceans*, *113*, C02S03. https://doi.org/10.1029/2005JC003384

Stroeve, J. C., Jenouvrier, S., Campbell, G. G., Barbraud, C., & Delord, K. (2016). Mapping and assessing variability in the Antarctic marginal ice zone, pack ice and coastal polynyas in two sea ice algorithms with implications on breeding success of snow petrels. *The Cryosphere*, *10*(4), 1823–1843. https://doi.org/10.5194/tc-10-1823-2016

Strong, C., & Rigor, I. G. (2013). Arctic marginal ice zone trending wider in summer and narrower in winter. *Geophysical Research Letters*, *40*, 4864–4868. https://doi.org/10.1002/grl.50928

Stuecker, M. F., Bitz, C. M., & Armour, K. C. (2017). Conditions leading to the unprecedented low Antarctic sea ice extent during the 2016 austral spring season. *Geophysical Research Letters*, *44*, 9008–9019. https://doi.org/10.1002/2017GL074691

Talley, L. D. (2013). WOCE atlas volume 4: Indian Ocean hydrographic web atlas. Lynne D. Talley. https://doi.org/10.21976/C61595

Turner, J., Phillips, T., Marshall, G. J., Hosking, J. S., Pope, J. O., Bracegirdle, T. J., & Deb, P. (2017). Unprecedented springtime retreat of Antarctic sea ice in 2016. *Geophysical Research Letters*, *44*, 6868–6875. https://doi.org/10.1002/2017GL073656

Uotila, J., Vihma, T., & Launiainen, J. (2000). Response of the Weddell Sea pack ice to wind forcing. *Journal of Geophysical Research - Oceans*, *105*(C1), 1135–1151. https://doi.org/10.1029/1999JC900265

Uotila, P., Vihma, T., Pezza, A. B., Simmonds, I., Keay, K., & Lynch, A. H. (2011). Relationships between Antarctic cyclones and surface conditions as derived from high-resolution numerical weather prediction data. *Journal of Geophysical Research-Atmospheres*, *116*(D7). https://doi.org/10.1029/2010JD015358

Valkonen, T., Vihma, T., & Doble, M. (2008). Mesoscale modeling of the atmosphere over Antarctic sea ice: A late-autumn case study. *Monthly Weather Review*, *136*(4), 1457–1474. https://doi.org/10.1175/2007MWR2242.1

Vihma, T., Launiainen, J., & Uotila, J. (1996). Weddell Sea ice drift: Kinematics and wind forcing. *Journal of Geophysical Research - Oceans*, *101*(C8), 18279–18296. https://doi.org/10.1029/96JC01441

Wadhams, P., Lange, M. A., & Ackley, S. F. (1987). The ice thickness distribution across the Atlantic sector of the Antarctic Ocean in midwinter. *Journal of Geophysical Research - Oceans*, *92*(C13), 14535–14552. https://doi.org/10.1029/JC092iC13p14535

Wadhams, P., Parmiggiani, F. F., de Carolis, G., Desiderio, D., & Doble, M. J. (2004). SAR imaging of wave dispersion in Antarctic pancake ice and its use in measuring ice thickness. *Geophysical Research Letters*, *31*, 15305. https://doi.org/10.1029/2004GL020340

WAMDI Group (1988). The WAM model—A third generation ocean wave prediction model. *Journal of Physical Oceanography*, *18*(12), 1775–1810. https://doi.org/10.1175/1520-0485(1988)018<1775:TWMTGO>2.0.CO;2

Wang, Y., Holt, B., Erick Rogers, W., Thomson, J., & Shen, H. H. (2016). Wind and wave influences on sea ice floe size and leads in the Beaufort and Chukchi Seas during the summer-fall transition 2014: WIND, WAVE, SEA ICE MORPHOLOGY. *Journal of Geophysical Research: Oceans*, *121*, 1502–1525. https://doi.org/10.1002/2015JC011349

Wang, Z., Turner, J., Sun, B., Li, B., & Liu, C. (2014). Cyclone-induced rapid creation of extreme Antarctic sea ice conditions. *Scientific Reports*, *4*(1), 5317. https://doi.org/10.1038/srep05317

Wei, J., Zhang, X., & Wang, Z. (2019). Impacts of extratropical storm tracks on Arctic sea ice export through Fram Strait. *Climate Dynamics*, *52*(3-4), 2235–2246. https://doi.org/10.1007/s00382-018-4254-8

Wei, L., & Qin, T. (2016). Characteristics of cyclone climatology and variability in the Southern Ocean. *Acta Oceanologica Sinica*, *35*(7), 59–67. https://doi.org/10.1007/s13131-016-0913-y

WMO (2014). *Guide to meteorological instruments and methods of observation* (Report No. WMO-No.8), (p. 1128). Genva, Switzerland: World Meteorological Organization. Retrieved from. http://hdl.handle.net/11329/365

Woods, C., & Caballero, R. (2016). The role of moist intrusions in winter Arctic warming and sea ice decline. *Journal of Climate*, *29*(12), 4473–4485. https://doi.org/10.1175/JCLI-D-15-0773.1

Worby, A. P., & Comiso, J. C. (2004). Studies of the Antarctic sea ice edge and ice extent from satellite and ship observations. *Remote Sensing of Environment*, *92*(1), 98–111. https://doi.org/10.1016/j.rse.2004.05.007

Ye, Y., Shokr, M., Heygster, G., & Spreen, G. (2016). Improving multiyear sea ice concentration estimates with sea ice drift. *Remote Sensing*, *8*(5), 397. https://doi.org/10.3390/rs8050397

Young, I. R., Zieger, S., & Babanin, A. V. (2011). Global trends in wind speed and wave height. *Science*, *332*(6028), 451–455. https://doi.org/10.1126/science.1197219

Yuan, N., Ding, M., Ludescher, J., & Bunde, A. (2017). Increase of the Antarctic sea ice extent is highly significant only in the Ross Sea. *Scientific Reports*, *7*(1), 41096. https://doi.org/10.1038/srep41096

Yuan, X., Patoux, J., & Li, C. (2009). Satellite-based midlatitude cyclone statistics over the Southern Ocean: 2. Tracks and surface fluxes. *Journal of Geophysical Research-Atmospheres*, *114*, D04106. https://doi.org/10.1029/2008JD010874

Zunz, V., Goosse, H., & Massonnet, F. (2013). How does internal variability influence the ability of CMIP5 models to reproduce the recent trend in Southern Ocean sea ice extent? *The Cryosphere*, *7*(2), 451–468. https://doi.org/10.5194/tc-7-451-2013